Rheologica Acta Rheol Acta 26:152–161 (1987)

The rotation of a suspended axisymmetric ellipsoid in a magnetic field

A. D. Shine and R. C. Armstrong

Department of Chemical Engineering and MIT-Industry Polymer Processing Program, Massachusetts Institute of Technology, Cambridge, Mass. (U.S.A.)

Abstract: Under the influence of a uniform and parallel magnetic field, a ferromagnetic fiber suspended in a Newtonian fluid rotates to align with the field direction. This study examines the field-induced rotation process for an individual non-Brownian axisymmetric ellipsoid suspended in a stagnant Newtonian fluid. Theoretical predictions are derived by a perturbation analysis for the limiting case where the strength of the applied magnetic field far exceeds the saturation magnetization of the ellipsoid. Numerical calculations are performed for the more general problem of an ellipsoid with known isotropic, non-hysteretic magnetic properties, using nickel and a stainless steel as examples. The analysis encompasses materials with field-induced, nonlinear magnetic properties, distinguishing these results from the simpler cases where the particle magnetization is either independent of, or linearly dependent on, the strength of the applied external field. In this study, predictions indicate that when the ellipsoid is magnetically saturated, the particle rotation is governed by the magnetoviscous time constant, $\tau_{MV} = \eta_s/\mu_0 M_s^2$. It is found that the rotation rate depends strongly on the aspect ratio, a/b, of the ellipsoid, but only weakly on the dimensionless magnetization, M_s/H_0.

Key words: Fiber suspension, magnetohydrodynamics, ferromagnetic particle, ellipsoid, rotation

Notation

A	geometric parameter for an ellipsoid, defined in eq. (2.5)
a, b	major, minor semi-axes of an axisymmetric ellipsoid
$\boldsymbol{D}$	demagnetization tensor for an ellipsoid
$\boldsymbol{D}^M$	magnetometric demagnetization tensor, the volume-average of $\boldsymbol{D}^P(\boldsymbol{r})$
$\boldsymbol{D}^P(\boldsymbol{r})$	position dependent demagnetization tensor, implicitly defined in eq. (2.12)
D_{xx}, D_{yy}, D_{zz}	demagnetization factors, the diagonal elements of $\boldsymbol{D}$. Values for ellipsoids are defined in eq. (2.15)
$\boldsymbol{F}^{(m)}$	magnetic force exerted on a body in a magnetic field
$\boldsymbol{H}_i; H_i$	magnetic field inside a ferromagnetic body; magnitude of $\boldsymbol{H}_i$
$\boldsymbol{H}_0; H_0$	magnetic field applied by external sources; magnitude of $\boldsymbol{H}_0$
$\boldsymbol{h}_i; h_{ix}, h_{iy}$	Cartesian components of dimensionless internal magnetic field, $\boldsymbol{h}_i = \boldsymbol{H}_i/H_0$
$\boldsymbol{I}$	moment of inertia tensor
k	geometric parameter for hydrodynamic resistance of a body rotating in a Newtonian fluid given in eq. (2.3)
$\boldsymbol{L}^{(h)}; L_z^{(h)}$	hydrodynamic torque exerted on a rotating body; the z-component of the hydrodynamic torque
$\boldsymbol{L}^{(m)}; L_z^{(m)}$	magnetic torque exerted on a magnetic body in a magnetic field, eq. (2.10); the z-component of the magnetic torque
$\boldsymbol{M}; M$	the magnetization, or dipole moment density, of a magnetic material; the magnitude of $\boldsymbol{M}$
M_s	the saturation value of M, approached by all ferromagnetic materials as H_i becomes large (figure 3)
m_s	the dimensionless saturation magnetization, M_s/H_0
$\boldsymbol{r}$	position vector of a point within a ferromagnetic body
s	dummy integration variable in eq. (2.5)
t	time
U	magnetoquasistatic potential energy of a magnetic body in a magnetic field, given in eq. (2.8)
u	curve-fitting variable in eq. (4.1); $u = \log H_i$
V	volume of a magnetic particle; for an axisymmetric ellipsoid, $V = (4/3)\pi a b^2$
x, y, z	rectangular coordinate axes fixed in the ellipsoid (figure 1)
β	angle of inclination of the major axis of the ellipsoid with respect to $\boldsymbol{H}_0$
η_s	viscosity of the Newtonian suspending medium
μ_0	the magnetic permeability of free space, $\mu_0 = 4\pi \cdot 10^{-7}$ H/m

τ_{MV} the magnetoviscous time constant, a characteristic time for a process involving a competition of viscous and magnetic stresses

χ the magnetic susceptibility of a magnetic material, $\chi = M/H_i$

$\boldsymbol{\Omega}; \Omega_z$ angular velocity of a rotating body; angular velocity about the z-axis of an ellipsoid, $\Omega_z = -d\beta/dt$

1. Introduction

An external electric or magnetic field provides a convenient non-invasive technique for applying a force or torque to particles in a suspension. The use of a magnetic field affords some experimental advantages over an electric field: (1) most fluids are non-magnetic, which gives the technique wide applicability and eliminates complications due to charge or polarization effects in the suspending medium, and (2) the absence of material breakdown effects permits the use of high field strengths and correspondingly high matrix fluid viscosities. The possible use of high fields and high viscosity fluids makes the study of magnetic fiber motion attractive for such practical applications as controlling fiber orientation for improved mechanical properties in polymeric composites or for inducing higher electrical conductivity in composites used for electromagnetic interference shielding purposes.

In order to achieve fiber orientation in a reasonable length of time, it is necessary to use strongly ferromagnetic materials such as iron, nickel, cobalt, or alloys of these. Ferromagnetic materials typically have nonlinear magnetic properties and can exhibit anisotropy and hysteresis as well, which distinguish them from dielectric particles with linear properties [1–4]. The problem considered here treats the magnetic moment in the particle as totally induced by the field, hence as susceptible to changes in the magnitude or orientation of the applied field. This is different than the problem of permanently magnetized particles, where the magnetization of the particle is fixed in magnitude and direction, independent of the applied field. However, even the magnetic moment of a permanently magnetized particle can change direction under the influence of a strong field, provided that the time required for orientation of the particle axis is long relative to the time required for reorientation of the internal magnetic moment [5]. This could occur if the particle were suspended in a high viscosity fluid, for instance, in the polymeric resins used in the manufacture of rubber magnets or in certain types of vertical magnetic recording media.

In this paper we present a calculation of the motion of a ferromagnetic ellipsoid suspended in a stagnant Newtonian fluid and subjected to the action of a uniform, parallel DC magnetic field. In the absence of inertial effects, the equation of motion for the ellipsoid is given by a simple torque balance; the balance is described in the next section. For the problem of an induced, nonlinear magnetic moment in the particle, a perturbation analysis is applied in section 3 for the limit of high field strength. Numerical solutions are required for arbitrary field strength, because of the coupled nature of the governing equations; examples are presented in section 4. In the final section, we summarize results and make a brief comparison between predictions of the motion from this analysis, and predictions for ellipsoids in which the magnetic moment is either linearly dependent on the applied field or permanent.

2. Equation of motion for a suspended magnetic ellipsoid

Consider a rigid, axisymmetric ellipsoid suspended in an unbounded Newtonian fluid and placed in a uniform, parallel, DC magnetic field, as shown in figure 1. The major axis (x-axis) of the ellipsoid is inclined at angle β relative to the external applied magnetic field,

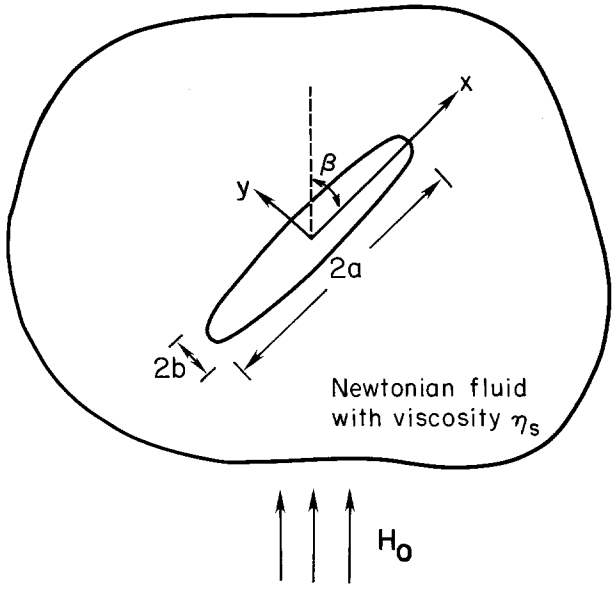

Fig. 1. A ferromagnetic ellipsoid is suspended in a Newtonian fluid with viscosity η_s. The suspension is subjected to a uniform magnetic field $\boldsymbol{H}_0$. The major and minor axes of the ellipsoid have lengths $2a$ and $2b$, respectively. The angle β denotes the inclination of the major axis of the ellipsoid with respect to the magnetic field direction. The z-axis is perpendicular to the plane of the diagram

$\boldsymbol{H}_0$. The assumption that the gravitational force on the fiber is negligible, together with the uniform, parallel field assumption, implies that no net force is acting on the particle. Therefore, the center of mass does not translate, and the rotation of the particle is given by a torque balance:

$$\boldsymbol{L}^{(m)} + \boldsymbol{L}^{(h)} = \frac{d}{dt}(\boldsymbol{I} \cdot \boldsymbol{\Omega}), \tag{2.1}$$

where $\boldsymbol{L}^{(m)}$ and $\boldsymbol{L}^{(h)}$ are the magnetic and hydrodynamic torques, respectively. The moment of inertia tensor of the ellipsoid is denoted by $\boldsymbol{I}$, and $\boldsymbol{\Omega}$ is the particle angular velocity.

When the fiber is free to rotate, under conditions of negligible particle inertia, the sum of the magnetic and hydrodynamic torques must vanish giving:

$$\boldsymbol{L}^{(m)} + \boldsymbol{L}^{(h)} = \boldsymbol{0}. \tag{2.2}$$

2.1 Hydrodynamic torque

The hydrodynamic torque on an axisymmetric, non-Brownian fiber with fore-aft symmetry suspended in a quiescent unbounded Newtonian fluid under conditions of Stokes flow has the simple form [6]:

$$\boldsymbol{L}^{(h)} = -k\,\eta_s\,\boldsymbol{\Omega}. \tag{2.3}$$

Here η_s is the viscosity of the Newtonian suspending fluid (η_s is used to avoid confusion with the symbol μ, which is conventionally understood to represent the magnetic permeability), $\boldsymbol{\Omega}$ is the angular velocity of the particle, and k is a parameter dependent solely on the geometry of the particle.

Expressions for the hydrodynamic torque at low Reynolds number on an ellipsoid suspended in an infinite Newtonian fluid have been derived for a quiescent fluid [7] and a fluid undergoing simple shear flow [8]. For an axisymmetric ellipsoid rotating at constant angular velocity $\boldsymbol{\Omega}$ about a minor axis in a stagnant Newtonian fluid with viscosity η_s, the hydrodynamic torque about the z-axis of the particle-fixed coordinate system shown in figure 1 is given by:

$$L_z^{(h)} = -\left(\frac{4}{3}\pi a b^2\right)\frac{4\eta_s[(a/b)^2+1]}{[2(a/b)^2(1-A)+A]}\Omega_z, \tag{2.4}$$

where the parameter A is given by the elliptic integral:

$$A = ab^2\int_0^\infty \frac{ds}{(s+a^2)^{1/2}(s+b^2)^{3/2}}. \tag{2.5}$$

For a prolate ellipsoid ($a > b$)

$$A = \frac{(a/b)^2}{(a/b)^2-1} - \frac{(a/b)\cosh^{-1}(a/b)}{[(a/b)^2-1]^{3/2}}, \tag{2.6}$$

whereas for an oblate ellipsoid ($b > a$)

$$A = \frac{(a/b)\cos^{-1}(a/b)}{[1-(a/b)^2]^{3/2}} - \frac{(a/b)^2}{1-(a/b)^2}. \tag{2.7}$$

The parameter A has a value of 2/3 for a sphere and approaches unity as $a/b \to \infty$.

In eq. (2.4) the volume of the ellipsoid, $(4/3)\pi ab^2$, has been separated from the rest of the front or "k" factor to emphasize that the hydrodynamic torque per unit volume is dependent upon the aspect ratio of the ellipsoid, but not on the absolute particle dimensions.

The effect of aspect ratio on the hydrodynamic torque per unit volume required to sustain a steady rotation rate Ω_z about a minor axis of the particle in a quiescent fluid is depicted in figure 2. The parameter k from eq. (2.3) has been scaled by the ellipsoid volume and is plotted on the ordinate. In the limit as $a/b \to \infty$, k/V for the ellipsoid approaches $2(a/b)^2/\ln(a/b)$. Figure 2 illustrates that the torque density required to sustain constant end-over-end rotation of an ellipsoid increases dramatically with increasing aspect ratio.

2.2 Magnetic torque

For a magnetoquasistatic system, the potential energy, U, of a magnetic body in an external magnetic

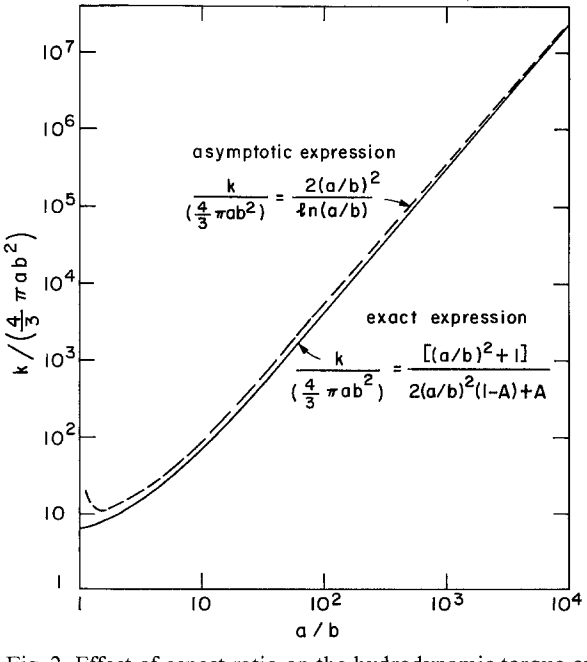

Fig. 2. Effect of aspect ratio on the hydrodynamic torque on a prolate ellipsoid suspended in a Newtonian fluid and rotating about a minor axis. The parameter k is defined in eq. (2.3). The solid line represents the exact expression in eq. (2.4) for a prolate ellipsoid; the dashed line gives the asymptotic expression. The parameter A is defined in eq. (2.5)

field, $\boldsymbol{H}_0$, is given by [9, 10]:

$$U = \frac{\mu_0}{2} \int_V (\boldsymbol{M} \cdot \boldsymbol{H}_0)\, dV, \tag{2.8}$$

where μ_0 is the permeability of free space ($= 4\pi \cdot 10^{-7}$ H/m), $\boldsymbol{M}$ is the magnetization, or dipole moment density, of the body at each point, and V is the volume of the body.

From this expression for energy, the force and torque exerted by the field on the magnetic particle can be calculated. The magnetic force, $\boldsymbol{F}^{(m)}$, is given by:

$$\boldsymbol{F}^{(m)} = -\nabla U = \mu_0 \int_V [\boldsymbol{M} \cdot \nabla \boldsymbol{H}_0]\, dV. \tag{2.9}$$

If the undisturbed field is uniform and parallel, $\nabla \boldsymbol{H}_0 = \boldsymbol{0}$, and there is no net magnetic force acting on the body. The magnetic torque $\boldsymbol{L}^{(m)}$ may be calculated by determining the change in energy resulting from a virtual rotation of the particle about a coordinate axis containing its midpoint. The torque exerted by the magnetic field on the body is:

$$\boldsymbol{L}^{(m)} = \mu_0 \int_V [\boldsymbol{M} \times \boldsymbol{H}_0]\, dV. \tag{2.10}$$

For a particle with a uniform, permanent magnetic moment fixed along the positive x-axis, eq. (2.10) simplifies to:

$$L_z^{(m)} = \mu_0 VMH_0 \sin\beta. \tag{2.11}$$

However, for a material with a non-permanent, induced magnetic moment, the magnetization is generally a nonlinear function of the magnetic field strength it experiences. This field inside the particle, denoted by $\boldsymbol{H}_i$, is dependent on, but different than, the external field $\boldsymbol{H}_0$. For a homogeneous, isotropic, non-hysteretic material, $\boldsymbol{M}$ and $\boldsymbol{H}_i$ are parallel, with $\boldsymbol{M}$ being a single-valued function of $\boldsymbol{H}_i$ that reaches a constant or saturation magnetization at high fields.

Typical features of the dependence of M on H_i for an initially unmagnetized ferromagnetic specimen, referred to as the initial magnetization curve, are shown in figure 3. Here M and H_i refer to the magnitudes of $\boldsymbol{M}$ and $\boldsymbol{H}_i$, respectively. Initially, M increases linearly with H_i, but only at very low field strengths. The (dimensionless) slope in this region is called the susceptibility of the material, and it is represented by the symbol χ. The linear region is followed by a magnetization regime characterized by a rapid increase of M with H_i. As H_i is further increased, the magnetization M approaches a constant or saturation value, M_s, where all the atomic magnetic moments are completely aligned in the field direction.

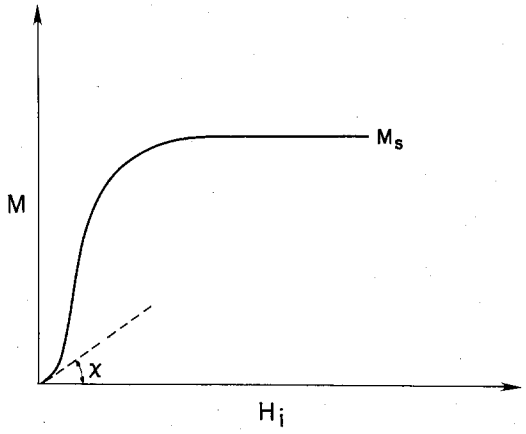

Fig. 3. Typical ferromagnetic magnetization curve. Here M and H_i are the magnitudes of the magnetization and internal magnetic field vectors, $\boldsymbol{M}$ and $\boldsymbol{H}_i$, respectively. The slope χ of $M(H_i)$ as $H_i \to 0$ is known as the susceptibility and the asymptotic value M_s of M as $H_i \to \infty$ is known as the saturation magnetization

In general, $\boldsymbol{H}_i$ and $\boldsymbol{M}$ are spatially varying within a particle, as well as dependent on particle shape, magnetic properties, and external field strength. Thus, evaluation of the integral in the magnetic torque expression, eq. (2.10), can be difficult. However, for the specific case of an ellipsoid, the solution of Maxwell's equations for a particle in an unbounded, uniform, parallel external field [9] shows that $\boldsymbol{H}_i$ is uniform and parallel. For an isotropic material, we note that $\boldsymbol{M}$ is therefore also uniform and parallel.

To determine the magnetic torque on a ferromagnetic ellipsoid, it is necessary to solve for $\boldsymbol{H}_i$ in order to determine $\boldsymbol{M}$ for use in eq. (2.10). The internal field can be expressed formally by means of the demagnetization tensor, $\boldsymbol{D}^P(\boldsymbol{r})$:

$$\boldsymbol{H}_i = \boldsymbol{H}_0 - \boldsymbol{D}^P(\boldsymbol{r}) \cdot \boldsymbol{M}. \tag{2.12}$$

Here $\boldsymbol{D}^P(\boldsymbol{r})$ is the position dependent demagnetization tensor, and $\boldsymbol{r}$ is the position vector for the location at which $\boldsymbol{H}_i$ is desired. The demagnetization tensor, which can be diagonalized for a suitable choice of coordinate system, is positive definite, symmetric, and has a trace of unity [11]. Eq. (2.12) predicts that the internal field of any ferromagnetic material will be less than the field that would exist in the absence of the material ($\boldsymbol{H}_0$). The magnetic material in effect opposes the applied field by setting up its own magnetic field in the opposite direction, $-\boldsymbol{D}^P(\boldsymbol{r}) \cdot \boldsymbol{M}$.

The volume average of the demagnetization tensor is called the magnetometric demagnetization tensor and is given by:

$$\boldsymbol{D}^M = \frac{1}{V} \int_V \boldsymbol{D}^P(\boldsymbol{r})\, dV, \tag{2.13}$$

where V is the volume of the particle. Since $\boldsymbol{H}_i$, $\boldsymbol{H}_0$, and $\boldsymbol{M}$ are constant throughout the volume of an isotropic, magnetic ellipsoid in a uniform, parallel, external field, $\boldsymbol{D}^P(\boldsymbol{r}) = \boldsymbol{D}^M$ for the instance considered here; hence we drop the superscripts and refer to the demagnetization tensor as $\boldsymbol{D}$. Eq. (2.12) is rewritten as:

$$\boldsymbol{H}_i = \boldsymbol{H}_0 - \boldsymbol{D} \cdot \boldsymbol{M} . \tag{2.14}$$

The diagonal components of $\boldsymbol{D}$ are known as the ellipsoidal demagnetizing factors and are given by [12]:

$$D_{xx} = 1 - A , \quad D_{yy} = D_{zz} = A/2 , \tag{2.15}$$

where A is given in eq. (2.5).

Eq. (2.14) can be interpreted physically as indicating that the internal field is influenced by competing tendencies to orient parallel to the applied field and also to orient parallel to the major axis of the ellipsoid, since the demagnetizing factor is lowest in this direction. The balance struck between these effects, which determines the internal field, is influenced by the strength and orientation of $\boldsymbol{H}_0$, as well as by the particle shape and magnetic properties.

Invoking the isotropy assumption which leads to parallel $\boldsymbol{M}$ and $\boldsymbol{H}_i$ and substituting the expression for $\boldsymbol{M}$ from eq. (2.14) transforms eq. (2.10) into:

$$\frac{L_z^{(m)}}{V} = \frac{\mu_0 H_0^2 M^2 (D_{yy} - D_{xx}) \sin\beta \cos\beta}{(H_i + D_{xx} M)(H_i + D_{yy} M)} . \tag{2.16}$$

The factor $(D_{yy} - D_{xx})$ is relatively constant for long prolate ellipsoids, having a value of 0.416 for $a/b = 5$ and increasing to 0.5 for infinitely long ellipsoids. In general, H_i and M in eq. (2.16) are not explicitly known since they are coupled through eq. (2.14) and the nonlinear material function $M = M(H_i)$.

However, at very low values of the applied field H_0 where $M = \chi H_i$, M can be eliminated from eq. (2.16) to yield

$$\frac{L_z^{(m)}}{V} = \frac{\mu_0 \chi^2 H_0^2 (D_{yy} - D_{xx}) \sin\beta \cos\beta}{(\chi D_{xx} + 1)(\chi D_{yy} + 1)} . \tag{2.17}$$

This is exactly analogous to the result for the electric torque on a dielectric particle in an electric field, although validity is restricted to small H_0, and no real magnetic material could have an infinite χ, in contrast to the electric analog of a perfect conductor.

2.3 *The magnetoviscous time constant, τ_{MV}*

By combining the expressions for the hydrodynamic and magnetic torques with the equation of motion, we obtain for a permanently magnetized ellipsoid:

$$\Omega_z = -\frac{d\beta}{dt} = \left(\frac{\mu_0 M H_0}{\eta_s}\right) \frac{[2(a/b)^2 (1 - A) + A] \sin\beta}{4[(a/b)^2 + 1]} , \tag{2.18}$$

which is easily integrated to give

$$\ln\tan[\beta(t)/2] - \ln\tan[\beta(0)/2] = -\left(\frac{\mu_0 M H_0}{\eta_s}\right) t \frac{2(a/b)^2 (1 - A) + A}{4[(a/b)^2 + 1]} . \tag{2.19}$$

For materials for which the magnetization is linear in the field strength the corresponding results are

$$\Omega_z = -\frac{d\beta}{dt} = \left(\frac{\mu_0 H_0^2}{\eta_s}\right) \cdot \frac{\chi^2 [(3A/2) - 1][2(a/b)^2 (1 - A) + A] \sin\beta \cos\beta}{4[\chi(1 - A) + 1][(\chi A/2) + 1][(a/b)^2 + 1]} \tag{2.20}$$

and

$$\ln\tan\beta(t) - \ln\tan\beta(0) = -\left(\frac{\mu_0 H_0^2}{\eta_s}\right) t \frac{[(3A/2) - 1][2(a/b)^2 (1 - A) + A] \chi^2}{4[\chi(1 - A) + 1][(\chi A/2) + 1][(a/b)^2 + 1]} . \tag{2.21}$$

In both these limiting cases, the time evolution of the orientation angle β has the form of $(t/\tau_{MV}) f(a/b, \chi)$, where τ_{MV} is referred to as the magnetoviscous time constant [13]; it represents a characteristic time for a process involving competition of viscous and magnetic stresses. For a material in the linear magnetization regime,

$$\tau_{MV\,(\text{linear})} = \eta_s / \mu_0 H_0^2 , \tag{2.22}$$

whereas for a permanently magnetized material

$$\tau_{MV\,(\text{permanent})} = \eta_s / \mu_0 M H_0 . \tag{2.23}$$

Even in an extremely viscous fluid, the magnetoviscous time constant can be relatively short when a moderate magnetic field is applied. For example, if we choose $\eta_s = 10^4$ Pa · s (typical of the zero-shear-rate viscosity of a polymer melt) and $H_0 = 8 \cdot 10^4$ A/m $= 10^3$ Oersteds (typical of the field available from an iron core electromagnet), then $\tau_{MV\,(\text{linear})}$ would be approximately 1 second. For most permanently magnetized materials $\tau_{MV\,(\text{permanent})}$ would be even smaller.

For the more general problem of a nonlinear, induced moment, however, the appropriate magnetoviscous time constant is not yet evident, since the equation of motion is:

$$\Omega_z = -\frac{d\beta}{dt} = -\frac{\mu_0 H_0^2 M^2 (D_{yy} - D_{xx}) [2(a/b)^2 (1 - A) + A] \sin\beta \cos\beta}{4\eta_s (H_i + D_{xx} M)(H_i + D_{yy} M)[(a/b)^2 + 1]} , \tag{2.24}$$

which is coupled with eq. (2.14) through the material magnetization function, $M = M(H_i)$. In the succeeding sections, eq. (2.24) will be solved by a perturbation method for large H_0, and solved numerically for field srengths in between the low-field, linear regime and the large H_0 limit.

3. Perturbation solution for $H_0 \gg M$

When an increasingly higher strength magnetic field is imposed, the magnetization of all ferromagnetic materials approaches the saturation magnetization, M_s. Saturation is generally considered to be achieved when magnetization reaches 98% or 99% of M_s. When a ferromagnetic material is magnetically saturated, the magnitude of $\boldsymbol{M}$ does not change with further increases in the magnetic field, although the direction of $\boldsymbol{M}$ in an isotropic material will adjust itself to be parallel with the internal field $\boldsymbol{H}_i$. Using M_s to denote the saturation magnetization and dividing the numerator and denominator in eq. (2.16) by H_0^2 leaves

$$\frac{L_z^{(m)}}{V} = \frac{\mu_0 M_s^2 (D_{yy} - D_{xx}) \sin\beta \cos\beta}{(h_i + D_{xx} m_s)(h_i + D_{yy} m_s)}, \tag{3.1}$$

where the lower case letters denote dimensionless quantities that have been scaled by H_0. Eq. (2.14) becomes:

$$h_{ix} = \cos\beta - D_{xx} m_s \frac{h_{ix}}{h_i}; \quad h_{iy} = \sin\beta - D_{yy} m_s \frac{h_{iy}}{h_i} \tag{3.2}$$

and

$$\begin{aligned} h_i^2 &= h_{ix}^2 + h_{iy}^2 \\ &= 1 - 2m_s (D_{xx} h_{ix} (\cos\beta)/h_i + D_{yy} h_{iy} (\sin\beta)/h_i) \\ &\quad + D_{xx}^2 m_s^2 h_{ix}^2/h_i^2 + D_{yy}^2 m_s^2 h_{iy}^2/h_i . \end{aligned} \tag{3.3}$$

If the parameter $m_s = M_s/H_0$ is taken to be small compared with unity, then eq. (3.1) can be expanded as a series in powers of m_s. Retaining terms up to order m_s^2 in this expansion [14] gives the denominator in eq. (3.1):

$$\begin{aligned} &(h_i + D_{xx} m_s)(h_i + D_{yy} m_s) = 1 \\ &+ m_s (D_{yy} - D_{xx})(\cos^2\beta - \sin^2\beta) \\ &+ 2m_s^2 [(D_{xx}^2 \cos^2\beta + D_{yy}^2 \sin^2\beta) \\ &\qquad - (D_{xx} \cos^2\beta + D_{yy} \sin^2\beta)^2] \\ &+ O(m_s^3) . \end{aligned} \tag{3.4}$$

In the lowest order approximation for very large H_0, the magnetic torque will have the same angular dependence, namely $\sin\beta \cos\beta$, as for the magnetically linear material. However, the magnetic torque scales as the square of the saturation magnetization for the large field strength limit, rather than as the square of the applied field strength, as in the linear limit. In the order 1 approximation, the entire geometric dependence of the magnetic torque term is contained in the relatively constant $(D_{yy} - D_{xx})$ factor.

When eqs. (3.1) and (3.4) are combined and the result equated with the hydrodynamic torque, the ellipsoid motion is determined to be at lowest order in m_s:

$$\begin{aligned} &\ln\tan\beta(t) - \ln\tan\beta(0) \\ &= -\left(\frac{\mu_0 M_s^2}{\eta_s}\right) t \left\{\frac{[2(a/b)^2 (1-A) + A][(3A/2) - 1]}{4[(a/b)^2 + 1]}\right\} . \end{aligned} \tag{3.5}$$

If terms through order m_s^2 are retained in eq. (3.4), then eq. (3.5) is modified as follows:

$$\begin{aligned} &\{\ln\tan\beta + m_s (D_{yy} - D_{xx})(\ln\sin\beta + \ln\cos\beta) \\ &\quad + 2m_s^2 (D_{xx}^2 \ln\sin\beta - D_{yy}^2 \ln\cos\beta) \\ &\quad - 2m_s^2 [D_{xx}^2 (\tfrac{1}{2}\cos^2\beta + \ln\sin\beta) + D_{yy} D_{xx} \sin^2\beta \\ &\qquad + D_{yy}^2 (-\tfrac{1}{2}\cos^2\beta + \ln\cos\beta)]\}_{\beta(0)}^{\beta(t)} \\ &= -\frac{\mu_0 M_s^2}{\eta_s} t \left\{\frac{[2(a/b)^2 (1-A) + A][(3A/2) - 1]}{4[(a/b)^2 + 1]}\right\} . \end{aligned} \tag{3.6}$$

From eqs. (3.5) and (3.6) we see that the magnetoviscous time constant in the limit $m_s \ll 1$ is

$$\tau_{MV(M_s/H_0 \ll 1)} = \eta_s/\mu_0 M_s^2 . \tag{3.7}$$

Table 1 lists some calculated times for an ellipsoid to rotate from $\beta = 75°$ to $\beta = 15°$ in a fluid with viscosity $\eta_s = 10^4$ Pa · s, obtained by using eq. (3.5). The times increase significantly as the ellipsoidal aspect ratio increases, since the { } term in eq. (3.5) varies roughly as $\ln(a/b)/(a/b)^2$ as a result of the dominance of the aspect ratio influence of the hydrodynamic torque expression (figure 2).

Table 1. Calculated*) times (in seconds) for a saturated ellipsoid to rotate from $\beta = 75°$ to $\beta = 15°$ in a fluid with $\eta_s = 10^4$ Pa · s

a/b	Nickel	416 stainless steel	Iron
10	15	2.0	1.2
20	45	6.1	3.6
50	210	29	17
100	730	99	59
200	2,500	340	200
500	14,000	1,800	1,100

*) Results were calculated from eq. (3.5) with M_s values of $4.9 \cdot 10^5$ A/m for nickel, $1.33 \cdot 10^6$ A/m for stainless steel, and $1.70 \cdot 10^6$ A/m for iron

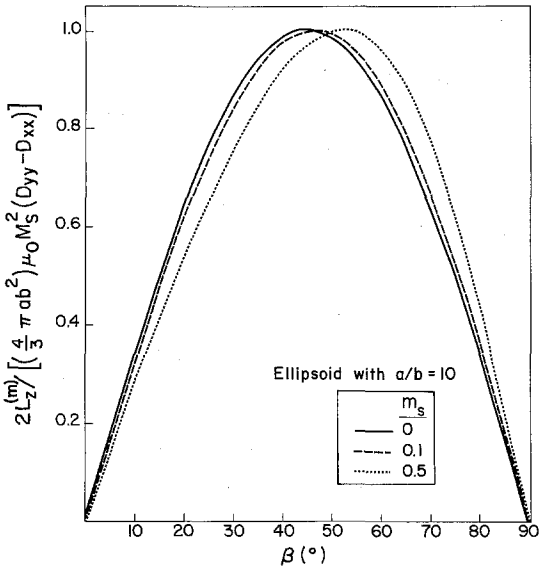

Fig. 4. Magnetic torque on a saturated ellipsoid for small values of $m_s = M_s/H_0$. The lines are calculated from the perturbation result obtained by combining eqs. (3.1) and (3.4); terms up to order m_s^2 were retained

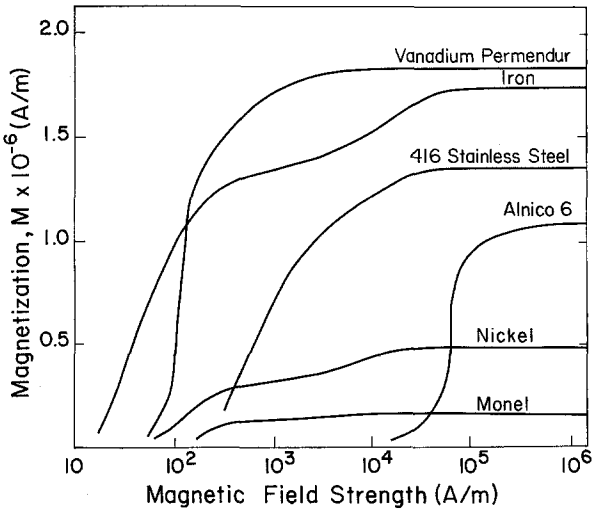

Fig. 5. DC magnetization curves for some ferromagnetic materials (taken from [15])

To gain some insight into the rotation behavior of magnetic fibers at large but finite applied fields, the higher order terms in m_s from eqs. (3.4) and (3.6) need to be considered. The perturbation expansion is rigorously valid only for $m_s \ll 1$ and only up to order m_s^2. Figure 4 shows the influence of m_s on the magnetic torque on an ellipsoid with $a/b = 10$ for the order m_s^2 approximation compared with the limit of vanishing m_s. The magnitude of the maximum magnetic torque experienced is virtually unaffected by the value of m_s; the major effect of m_s seems to be in shifting the angular location of the maximum torque to higher β, i.e., to orientations further out of alignment with the field.

Although eqs. (3.4) and (3.6) are restricted to relatively high values of H_0, so that $M_s/H_0 \ll 1$, the saturation magnetization of a ferromagnetic material such as a long nickel ellipsoid can be reached at a value of $M_s/H_0 > 10$. Thus, it is desirable to investigate situations where somewhat lower values of H_0 are permissible; however, this necessitates using a numerical approach, as described in the next section.

4. Numerical calculation of the motion of a ferromagnetic ellipsoid

For situations other than the limiting cases described above, the ellipsoid orientation cannot be determined analytically because of the nonlinear nature of the equations involved. Thus, a numerical approach is used to solve for the magnetic torque. This numerical method is applicable for either linear or saturated materials, or for any magnetization curve which passes through $\boldsymbol{H}_i = \boldsymbol{0}$, $\boldsymbol{M} = \boldsymbol{0}$ and which can be expressed analytically. In this paper, stainless steel 416 is used as an example.

The magnetic constitutive relation, $M(H_i)$, for stainless steel 416 is shown in figure 5 along with similar curves for several other ferromagnetic materials. A fifth order polynomial was fit to data points from the literature [15]; the result is

$$M = 7.9577 \cdot 10^4 (-306.1506 + 316.695u - 128.444u^2 + 26.5621u^3 - 2.76744u^4 + 0.115186u^5), \quad (4.1)$$

where $u = \log H_i$, and both M and H_i are expressed in A/m. This expression is valid over the range $H_i =$ 400 A/m to $H_i = 6.9 \cdot 10^4$ A/m; above the higher value of H_i, the saturation magnetization of $1.33 \cdot 10^6$ A/m was used.

Eq. (4.1) along with eq. (2.14) was used in a Newton-Raphson iteration procedure [16] to determine $\boldsymbol{M}$ and $\boldsymbol{H}_i$, using H_0, β, D_{xx} and D_{yy} as parameters. The calculated values where then substituted into the equation of motion to determine the angular velocity Ω_z as a function of the orientation angle β; this expression could be subsequently integrated to give β as a function of time. The arbitrary integration constant was chosen by assigning $\beta = 45°$ at $t = 0$.

Results for the angular velocity calculation are illustrated in figure 6 for an ellipsoid with $a/b = 20$ and suspended in a fluid with $\eta_s = 10^4$ Pa · s. Curve 6a represents the limit of infinitely large applied field

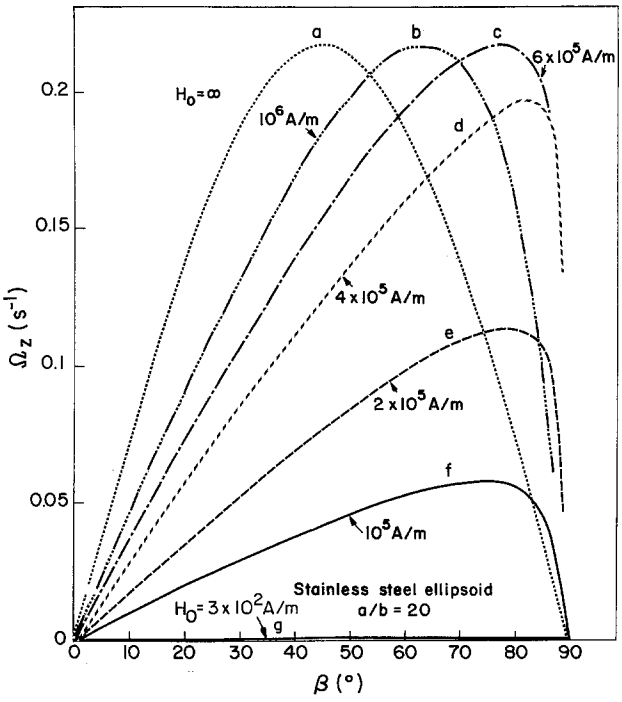

Fig. 6. Rotation rate of a ferromagnetic ellipsoid suspended in a Newtonian fluid with $\eta_s = 10^4$ Pa · s. Curves a–g show the influence of varying the external field strength on the particle motion. The curves were calculated for stainless steel with M given by eq. (4.1) and with $D_{xx} = 6.75 \cdot 10^{-3}$, $D_{yy} = 0.4966$

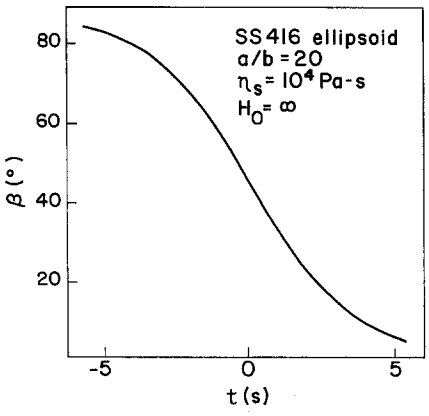

Fig. 7. Calculated orientation angle, β, as a function of time for a ferromagnetic ellipsoid rotating in an unbounded Newtonian fluid with viscosity η_s. The aspect ratio for the ellipsoid is $a/b = 20$ and its magnetic properties are taken to be those of stainless steel 416, cf. eq. (4.1). The fluid viscosity is $\eta_s = 10^4$ Pa · s and the external magnetic field strength is very large, $H_0 \to \infty$. The curve is calculated as described in section 4, with the arbitrary integration constant chosen as $\beta(t=0) = 45°$

strength; as expected, the numerical procedure gives the same result as the perturbation approximation derived in section 3. Curves 6b and 6c are calculated for values of m_s (1.33 and 2.22, respectively) outside the range of validity of the perturbation approach. For both of these curves the fields are sufficiently strong to produce saturation. The trends observed for lower values of m_s are also exhibited in these curves, namely (1) that the magnitude of the maximum angular velocity (or magnetic torque) is independent of applied field strength, and (2) that maximum rotation rates are achieved at higher values of β as the field strength is lowered, provided that the magnetization is at the saturation limit.

However, once the applied field value drops below that required to maintain saturation of the magnetization of the ellipsoid, as occurs in curves 6d, 6e, and 6f, the maximum angular velocity decreases with decreasing H_0, and the location of the maximum shifts back towards 45°. Ultimately, when the applied field is sufficiently low that the magnetization in the ellipsoid is linear in the applied field strength, the angular velocity of the ellipsoid will exhibit the features of the analytical solutions discussed in section 2. If the linear field limit for stainless steel is estimated at 300 A/m, with $\chi = 500$, the maximum of curve 6g is only $\Omega_z = 2.5 \cdot 10^{-6}\,s^{-1}$.

An interesting feature exhibited in figure 6 is that when the applied field is high enough to ensure magnetic saturation, a higher value of the applied field will actually result in lower rotation rates at high angles. Thus, for saturated ferromagnetic ellipsoids more than 45° out of alignment with the field, there exists an optimum value of applied field to produce a maximum particle rotation rate.

When the calculated angular velocities are numerically integrated, the ellipsoid orientation can be determined as a function of time. Such a $\beta = \beta(t)$ function, corresponding to curve 6a, is shown in figure 7. All such curves are characteristically sigmoidal, because of the necessary zero slope at $\beta = 90°$ (unstable equilibrium) and $\beta = 0°$ (stable equilibrium). Since such curves are ill-suited for quantitative comparison with experimental data, figure 8 shows the fiber orientation as the function $\ln \tan \beta$, the characteristic function for both the constant permeability and high field saturation limits. Here, β is arbitrarily considered to be 45° when $t = 0$. In such a plot, differences in orientation for different field strengths are difficult to determine above $\beta = 45°$, because the curves are close together and are curved. However, at lower orientation angles, the plots of $\ln \tan \beta$ vs. t yield straight lines with steeper slopes at higher applied field strengths, thereby suggesting a useful means of quantitative comparison between experimental results and theoretical predictions. The slope is of course influenced by the magnetoviscous time constant and the aspect ratio.

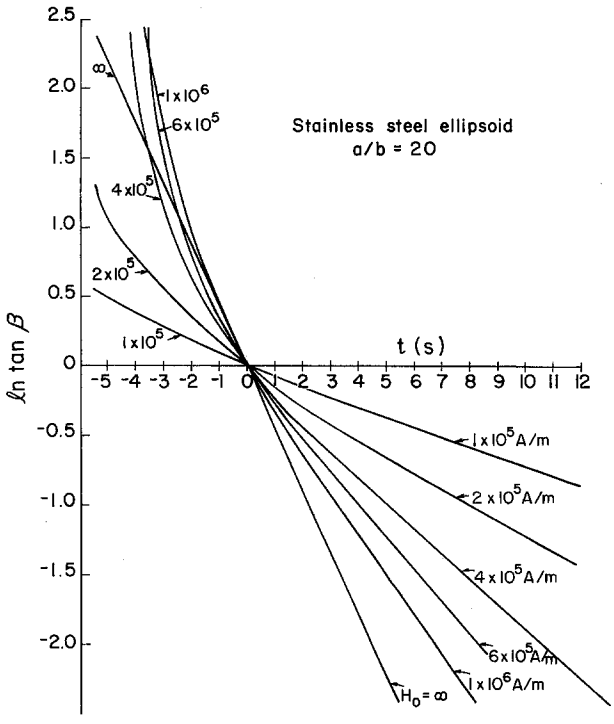

Fig. 8. Calculated orientation angle β as a function of time for a ferromagnetic ellipsoid rotating in an unbounded, quiescent Newtonian fluid. All conditions are the same as in figure 7 except that several values of the external magnetic field strength H_0 have been used as indicated. The usefulness of the ln tan function for presenting these results is seen in the large linear region of the curves for long times (small β). The arbitrary integration constant is chosen so that $\beta(t=0) = 45°$

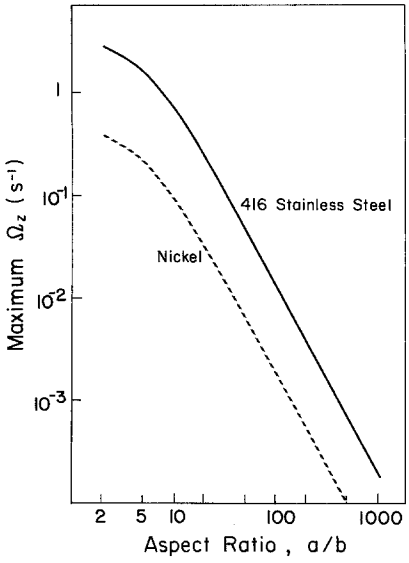

Fig. 9. Calculated maximum rotation rate, Ω_z, as a function of aspect ratio for an ellipsoid which has the magnetic properties of stainless steel 416 or nickel and which is suspended in a Newtonian fluid with $\eta_s = 10^4$ Pa · s. The maximum Ω_z is the angular velocity experienced by the ellipsoid at $\beta = 45°$ and $H_0 \to \infty$:

$$\Omega_{z,(\max)} = \left(\frac{\mu_0 M_s^2}{\eta_s}\right)\left\{\frac{(3A-2)\,[2\,(a/b)^2\,(1-A)+A]}{16\,[(a/b)^2+1]}\right\},$$

where A is defined in eq. (2.5)

Although specifics of the magnetization curve differ for different ferromagnetic materials, if an ellipsoid is magnetically saturated, the orientation function $\beta = \beta(t/\tau_{MV})$ is dependent only on the fiber aspect ratio and the dimensionless magnetization $m_s = M_s/H_0$. Thus, for equal values of a/b and m_s, the (dimensional) angular velocities of two ellipsoids will differ only by τ_{MV}. Figure 9 provides a graphic comparison of the maximum angular velocity experienced by saturated nickel and stainless steel ellipsoids suspended in a fluid with $\eta_s = 10^4$ Pa · s. Rotation rates drop off dramatically with increasing a/b, because of the influence of the hydrodynamic torque term.

5. Summary

The following assumptions have been used in the derivation of expressions for the rotation of a suspended axisymmetric ellipsoid in a magnetic field:

(1) Particle inertia and Brownian motion are negligible, so that a simple torque balance expresses the equation of motion.
(2) The suspending fluid is Newtonian.
(3) The undisturbed fluid is stagnant and unbounded.
(4) Fluid inertia is negligible.
(5) The particle is homogeneous and has isotropic magnetic properties.
(6) The undisturbed applied DC magnetic field is uniform and parallel and extends to infinity.
(7) The particle is initially unmagnetized and is non-hysteretic.
(8) The particle magnetization instantaneously adjusts itself to its equilibrium value.

The magnetoviscous time constant, τ_{MV}, the characteristic time for motion resulting from competition of viscous and magnetic stresses, was found to vary significantly depending on the mechanism for producing the magnetic stresses. For three separate magnetic regimes, τ_{MV} was shown to be: (1) $\eta_s/\mu_0 H_0^2$ for constant magnetic permeability, analogous to a dielectric material [17, 18]; (2) $\eta_s/\mu_0 M_s H_0$ for a permanently magnetized particle; and (3) $\eta_s/\mu_0 M_s^2$ for an isotropic material with an induced saturation moment. Under practical conditions, H_0 and M_s may differ by orders of magnitude, so the proper choice of τ_{MV} is significant for scaling particle motion.

A convenient function for representing the rotation of the suspended ellipsoid is the $\ln \tan \beta$ function, which is the characteristic function at both the low field, linear limit as well as the high field, saturated limit. Even at intermediate field strengths, straight line plots of $\ln \tan \beta$ vs. t resulted for values of β less than 35°.

For an ellipsoid with an induced, saturated moment, the maximum rate of rotation is independent of the magnitude of the applied field, and the overall fiber alignment time increases only slightly with increasing applied field strength, in marked contrast to the motion of an ellipsoid with a permanently saturated moment. As the ellipsoidal aspect ratio is increased, however, the orientation process takes significantly longer, because of the dominance of the aspect ratio term arising in the hydrodynamic torque expression.

For a strongly ferromagnetic material, such as iron or steel, the characteristic fiber alignment time in a quiescent fluid with $\eta_s = 10^4$ Pa · s would be of the order of 10 s for an ellipsoid with $a/b = 20$. This suggests that a magnetic field could be successfully used to orient magnetic fibers in a high viscosity melt or suspension, within a practically feasible time frame.

Acknowledgements

The authors would like to acknowledge the MIT-Industry Polymer Processing Program for financial support of this work.

References

1. Chaffey CE, Mason SG (1964) J Coll Int Sci 19:525
2. Okagawa A, Fox RG, Mason SG (1974) J Coll Int Sci 47:536
3. Okagawa A, Mason SG (1974) J Coll Int Sci 47:568
4. Arp PA, Foister RT, Mason SG (1980) Adv Coll Int Sci 12:295
5. Charles SW, Popplewell J (1980) In: Wohlfarth EP (ed), Ferromagnetic Materials, Volume 2, North-Holland Publishing Co, New York, p 546.
6. Brenner H (1963) Chem Eng Sci 18:1
7. Edwardes D (1892) Quart J Math 26:70
8. Jeffery GB (1922) Proc Roy Soc (London) A 102:161
9. Stratton JA (1941) Electromagnetic Theory, McGraw-Hill, New York
10. Cowan EW (1968) Basic Electromagnetism, Academic Press, New York
11. Moskowitz R, Della Torre E (1966) IEEE Trans Magn 2:739
12. Brown WF (1962) Magnetostatic Principles in Ferromagnetism, North-Holland Publishing Co, Amsterdam
13. Melcher JR (1981) Continuum Electromechanics, MIT Press, Cambridge, Mass.
14. Shine AD (1982) The Rotation of Suspended Ferromagnetic Fibers in a Magnetic Field, PhD Thesis, Massachusetts Institute of Technology, p 214
15. Electrical Materials Handbook (1961) Allegheny Ludlum Steel Corporation, p III/2
16. Dahlquist G, Björk Å (1974) Numerical Methods, Prentice-Hall, Englewood Cliffs, New Jersey, p 249
17. Demetriades ST (1958) J Chem Phys 29:1054
18. Allan RS, Mason SG (1962) Proc Roy Soc (London) A 267:62

(Received April 22, 1986)

Authors' addresses:

Prof. A. D. Shine
Department of Chemical Engineering
and Petroleum Refining
Colorado School of Mines
Golden, CO 80401 (U.S.A.)

Prof. R. C. Armstrong*)
Department of Chemical Engineering
Massachusetts Institute of Technology
Cambridge, MA 02139 (U.S.A.)

*) To whom correspondence should be addressed